Evaluation of Implicit and Explicit Wave Dissipation Models for Submerged and Emergent Aquatic Vegetation

Ascencio, Jaime A.; Jacobsen, Niels G.; McFall, Brian C.; Groeneweg, Jacco; Vuik, Vincent; Reniers, Ad J.H.M.

DOI
10.2112/JCOASTRES-D-21-00110.1

Publication date
2022

Document Version
Final published version

Published in
Journal of Coastal Research

Citation (APA)
Ascencio, J. A., Jacobsen, N. G., McFall, B. C., Groeneweg, J., Vuik, V., & Reniers, A. J. H. M. (2022). Evaluation of Implicit and Explicit Wave Dissipation Models for Submerged and Emergent Aquatic Vegetation. *Journal of Coastal Research*, *38*(4), 807-815. https://doi.org/10.2112/JCOASTRES-D-21-00110.1

Evaluation of Implicit and Explicit Wave Dissipation Models for Submerged and Emergent Aquatic Vegetation

Authors: Ascencio, Jaime A., Jacobsen, Niels G., McFall, Brian C., Groeneweg, Jacco, Vuik, Vincent, et al.

Source: Journal of Coastal Research, 38(4) : 807-815

Published By: Coastal Education and Research Foundation

URL: https://doi.org/10.2112/JCOASTRES-D-21-00110.1

Journal of Coastal Research	38	4	807–815	Coconut Creek, Florida	July 2022

Evaluation of Implicit and Explicit Wave Dissipation Models for Submerged and Emergent Aquatic Vegetation

Jaime A. Ascencio[†], Niels G. Jacobsen[‡§], Brian C. McFall[††]*, Jacco Groeneweg[‡], Vincent Vuik[‡‡§§], and Ad J.H.M. Reniers[‡‡]

[†]Reefy
Delft, The Netherlands

[‡]Deltares
Delft, The Netherlands

[§]Vattenfall
Copenhagen, Denmark

[††]U.S. Army Engineer, Research, and Development Center
Vicksburg, MS 39180, U.S.A.

[‡‡]Department of Hydraulic Engineering
Delft University of Technology
Delft, The Netherlands

[§§]HKV Consultants
Lelystad, The Netherlands

www.cerf-jcr.org

www.JCRonline.org

ABSTRACT

Ascencio, J.A.; Jacobsen, N.G.; McFall, B.C.; Groeneweg, J.; Vuik, V., and Reniers, A.J.H.M., 2022. Evaluation of implicit and explicit wave dissipation models for submerged and emergent aquatic vegetation. *Journal of Coastal Research,* 38(4), 807–815. Coconut Creek (Florida), ISSN 0749-0208.

To address the important research question of whether implicit (bottom friction) or explicit (stem drag) dissipation models are most appropriate for the prediction of wave attenuation due to aquatic vegetation, the Simulating Waves Nearshore (SWAN) spectral wave model has been extended with an explicit frequency-dependent dissipation model for submerged and emergent vegetation. The new explicit model is compared to existing explicit and implicit dissipation models in SWAN, and the distinguishing features of each of the dissipation models are quantified. The present work verifies the implementation of the new and existing dissipation models, outlines their distinguishing features, and compares model predictions against experimental data. The emphasis is on the transformation of the spectral wave periods $T_{m0,1}$ and $T_{m-1,0}$ over a canopy. Model evaluation based on academic and laboratory cases allows for recommendations regarding applicability of the three dissipation models, where the new method has the broadest applicability, since it bridges the gap in applicability between the other two dissipation models. The implementation of Jacobsen, McFall, and van der A (2019; A frequency distributed dissipation model for canopies; *Coastal Engineering*, 150, 135–146) is publicly available in SWAN version 41.31B.

ADDITIONAL INDEX WORDS: *Vegetated canopies, spectral energy dissipation, SWAN.*

INTRODUCTION

The understanding of wave attenuation by aquatic vegetation has steadily increased over the past decades with a combined effort based on field (Jadhav, Chen, and Smith, 2013; Nowacki, Beudin, and Ganju, 2017) and laboratory measurements (Anderson and Smith, 2014; Möller *et al*., 2014; Ozeren, Wren, and Wu, 2014) and development of modeling tools (Chen and Zhao, 2012; Hu *et al*., 2021; Mendez and Losada, 2004). The societal goal is to better understand the ecological and morphological system in the presence of vegetation and, furthermore, to account for the impact of vegetation on flood risk (Vuik *et al*., 2018). Here, the wave transformation in terms of both bulk spectral parameters and the shape of the spectrum is important for wave run-up and overtopping estimation (EurOtop, 2018). The developed models vary in degree of complexity, where the most advanced models are stem-resolving, intrawave models through a direct solution of the Reynolds-averaged Navier-Stokes equations for both rigid and flexible stems (Chang *et al*., 2017; Chen and Zou, 2019). Reduced model complexity is found in, for instance, XBeach (Van Rooijen *et al*., 2016) and SWASH (Suzuki *et al*., 2019; Van Rooijen *et al*., 2020), where the loads on the stems are parameterized through force coefficients, while wave nonlinearity is retained in the model formulation. Other models have been recently developed that apply cantilever-beam models to account for vegetation flexibility (Hu *et al*., 2021; Zhu *et al*., 2020). The advanced modeling approaches outlined above are useful for investigation of wave attenuation over complex bed profiles, mean velocity profiles, or swaying of vegetation; however, they are not useful for large-scale, regional wave transformation studies because of computational inefficiency and complexity of required inputs. Instead, spectral wave models are a more suitable approach because of the possibility to include wind input and reduce the computational burden. The modeling of wave dissipation by vegetation is included by implicit or explicit descriptions of the vegetation, where implicit effectively means that the dissipation is incorporated through an increased bed roughness, while explicit means the vertical characteristic of the vegetation (height, density, stiffness, *etc.*) is taken into account. There is an ongoing debate on whether implicit or explicit models perform the best with respect to the wave transformation in nearshore areas (see, *e.g*., Baron-Hyppolite *et al*., 2019; Nowacki, Beudin, and Ganju, 2017). The present study further addresses this

DOI: 10.2112/JCOASTRES-D-21-00110.1 received 24 August 2021; accepted in revision 11 January 2022; corrected proofs received 16 February 2022; published pre-print online 3 March 2022.
*Corresponding author: Brian.C.McFall@usace.army.mil

topic through comparison with analytical expressions and experimental data. The aim is achieved by comparing the performance of two explicit models (Jacobsen, McFall, and Van der A, 2019; Suzuki *et al*., 2012) and one implicit model (Collins, 1972) all available in SWAN, which leads to a quantification of the distinguishing features of the individual models. The models are first described in the "Methods" section, and then the model implementations are compared and verified in the "Results" section over a range of nondimensional depths to span natural canopies from deep-water kelp forests to shallow seagrass and emergent vegetation. Descriptions and evaluation of the unique features of the dissipation models are presented, and a recent experimental data set for attenuation over a long canopy consisting of rigid stems is used to quantify the accuracy with which spectral wave periods are predicted. The paper closes with discussion and conclusions.

METHODS

SWAN is a third-generation spectral wave model for the generation and transformation of wind waves in coastal waters (Booij, Ris, and Holthuijsen, 1999). In the present work, steady-state computations with a single dissipation term due to vegetation and no current are considered:

$$\frac{\partial c_{g,x}N}{\partial x}+\frac{\partial c_{g,y}N}{\partial y}+\frac{\partial c_{\theta}N}{\partial \theta}=\frac{S_v}{\sigma} \tag{1}$$

Here, $N = E/\sigma$ is the action density spectrum, E is wave energy density, σ is the intrinsic frequency, c_g is the group velocity per frequency along the horizontal spatial dimensions x and y, c_θ is the propagation velocity giving rise to refraction, θ is the wave direction, and S_v is the energy dissipation term due to vegetation. Three alternatives for S_v are described in the following sections. Tests of all three dissipation models have been applied in two-dimensional computations (Ascencio, 2020), though the present quantification of model performance is achieved with academic cases and experimental flume tests, so all computations were performed in 1D mode.

Collins (1972)—Implicit Approach

The dissipation due to vegetation using Collins (1972) assumes that all dissipation occurs as bottom friction. This takes the form:

$$S_{v,C-72}(\sigma,\theta)=-C_f U_{\mathrm{rms}} g\left(\frac{\sigma}{g\sinh kh}\right)^2 E(\sigma,\theta) \tag{2}$$

where g is the acceleration due to gravity, k is the wave number, h is the water depth, and C_f is a dimensionless friction coefficient. U_{rms} is the root-mean-square velocity at the seabed, which relates as follows to the energy spectrum using linear wave theory:

$$U_{\mathrm{rms}}^2=\left\langle\frac{\sigma^2}{\sinh^2 kh}E\right\rangle_{\sigma,\theta} \tag{3}$$

Here, $\langle\cdot\rangle_{\sigma,\theta}$ means integration over the frequency and directional space.

Suzuki *et al.* (2012)—Explicit Approach

Suzuki *et al*. (2012) presented a dissipation model for arbitrary wave spectra, where their starting point was the narrow-banded spectral dissipation model proposed by Mendez and Losada (2004).

Their dissipation term reads:

$$S_{v,S-12}(\sigma,\theta)=-\sqrt{\frac{2}{\pi}}g^2 C_D b_v N_v\left(\frac{\tilde{k}}{\tilde{\sigma}}\right)^3\frac{\sinh^3\tilde{k}h_v+3\sinh\tilde{k}h_v}{3\tilde{k}\cosh^3\tilde{k}h}\sqrt{E_{\mathrm{tot}}}E(\sigma,\theta) \tag{4}$$

where C_D is a tunable bulk drag coefficient, b_v is the frontal width of the stem, N_v is the number of stems per unit area, h_v is the vegetation height, and

$$E_{\mathrm{tot}}=\langle E(\sigma,\theta)\rangle_{\sigma,\theta} \tag{5}$$

is the total variance of the surface elevation. The key approximation of Suzuki *et al*. (2012) is to characterize the vertical velocity profile by a single characteristic relative frequency $\tilde{\sigma}$, and a single characteristic wave number $\tilde{k}$ which are defined as (WAMDI Group, 1988):

$$\tilde{\sigma}=\frac{E_{\mathrm{tot}}}{\langle\sigma^{-1}E(\sigma,\theta)\rangle_{\sigma,\theta}},\quad \tilde{k}=\frac{E_{\mathrm{tot}}^2}{\langle k^{-1/2}E(\sigma,\theta)\rangle_{\sigma,\theta}^2} \tag{6}$$

Here, $\tilde{\sigma}$ can be recognized as the bulk frequency based on the $T_{m-1,0}=m_{-1}/m_0$ wave period, where

$$m_i=\langle\sigma^i E(\sigma,\theta)\rangle_{\sigma,\theta} \tag{7}$$

is the ith moment of the energy spectrum. However, as discussed in Ascencio (2020), the current implementation in SWAN is based on $T_{m0,1}=m_0/m_1$. The extension of Mendez and Losada (2004) to broad spectra is based on a bulk energy dissipation, with the assumption of a distribution of dissipation over the individual frequency bins proportional to the spectral energy in each frequency bin: $S_{v,S-12}(\sigma,\theta)/E(\sigma,\theta)=\text{constant}$.

Jacobsen, McFall, and Van der A (2019)—Explicit Approach

Jacobsen, McFall, and Van der A (2019) have shown that the explicit model of Suzuki *et al*. (2012) gives a skewed bias in the dissipation with too high dissipation on the high frequencies and too little dissipation on the low frequencies, since in reality a long wave feels the vegetation more than a short wave. The bias originates from the choice of $S_{v,S-12}(\sigma,\theta)/E(\sigma,\theta)=$ constant. Jacobsen, McFall, and Van der A (2019) proposed and analyzed a dissipation model where the distribution of dissipation over frequencies and an upper cut-off frequency are implicitly incorporated by accounting for the shape of the velocity profile for each frequency:

$$S_{v,J-19}(\sigma,\theta)=-\frac{C_D}{g}b_v N_v\alpha_u^3\left\langle\left(\frac{\sigma\cosh k(z+h)}{\sinh kh}\right)^2\sqrt{\frac{2m_{u0}}{\pi}}E(\sigma,\theta)\right\rangle_{h_v} \tag{8}$$

Here, the integration refers to the vertical submerged part of the vegetation stem and the integral is approximated using Simpson's rule to within an accuracy of 1% for $kh<3$ (see Jacobsen, McFall, and Van der A, 2019, their appendix A on the accuracy of the numerical integration scheme). The coefficient α_u is incorporated to account for a velocity reduction within the

stems, since it was hypothesized by Jacobsen, McFall, and Van der A (2019) that single-stem drag coefficients can be applied, provided that appropriate and possibly frequency-dependent values of α_u are adopted. In the present work, $\alpha_u = 1$ is assumed. Furthermore,

$$m_{u0}(z) = \left\langle \left(\frac{\sigma \cosh k(z+h)}{\sinh kh} \right)^2 E(\sigma,\theta) \right\rangle_{\sigma,\theta} \tag{9}$$

is the zeroth moment of the horizontal velocity spectrum at level z. The hyperbolic functions in Equations (8) and (9) follow from linear wave theory and transform the wave energy spectrum to the velocity spectrum for waves in arbitrary depth (*e.g.*, Holthuijsen, 2007). Jacobsen, McFall, and Van der A (2019) proposed that the high-frequency cut-off has full effect when $f_{co}^2 = g/(4\pi(h - h_v))$, which is the frequency at which the corresponding wavelength is twice the nonvegetated part of water column: $h - h_v$.

The method by Jacobsen, McFall, and Van der A (2019) is released as part of the publicly available SWAN as of version 41.31B.

Comparison of Spectral Shape of S_v

The variation in the spectral dissipation shape for the three models is depicted in Figure 1 for two values of $k_p h$ (1.5 and 3) and two values of the vegetation height h_v/h (0.25 and 0.75). Subscript p refers to the peak wave period. Note that magnitudes of the bulk dissipation are addressed in a subsequent section. To better understand the range shown in Figure 1, the two $k_p h$ values of 1.5 and 3 correspond to peak periods (T_p) of 1.7 s and 1.2 s, respectively, in a 1 m water depth. The two upper panels show that an increase in $k_p h$ leads to a shift in the peak of the dissipation toward lower values of f for the Collins (1972) and Jacobsen, McFall, and Van der A (2019) models. Furthermore, the model by Collins (1972) dissipates the majority of the energy on $f < f_p$ for $k_p h = 3.0$, since the higher frequencies in the spectra have minor, if any, interaction with the bed.

The two bottom panels illustrate the effect of decreasing vegetation height from $h_v/h = 0.75$ to $h_v/h = 0.25$. The normalized dissipation is identical for the Collins (1972) and Suzuki *et al.* (2012) models, because of the proportionality to $E(\sigma,\theta)$in both models, while Jacobsen, McFall, and Van der A (2019) changes shape and becomes almost identical to the implicit formulation for $h_v/h = 0.25$. The excessive dissipation of the high frequencies for the Suzuki *et al.* (2012) model is clear in all panels.

RESULTS

The explicit and implicit dissipation models are quantitatively compared using analytical and experimental methods. The variations in frequency-dependent dissipation between models, noted in the "Methods" section, are captured by analyzing the bulk dissipation.

Regular Wave Dissipation

Simulations were performed with regular waves (a single frequency bin), and it was found that the results with the formulations by Suzuki *et al.* (2012) and Jacobsen, McFall, and Van der A (2019) were identical. This is in line with

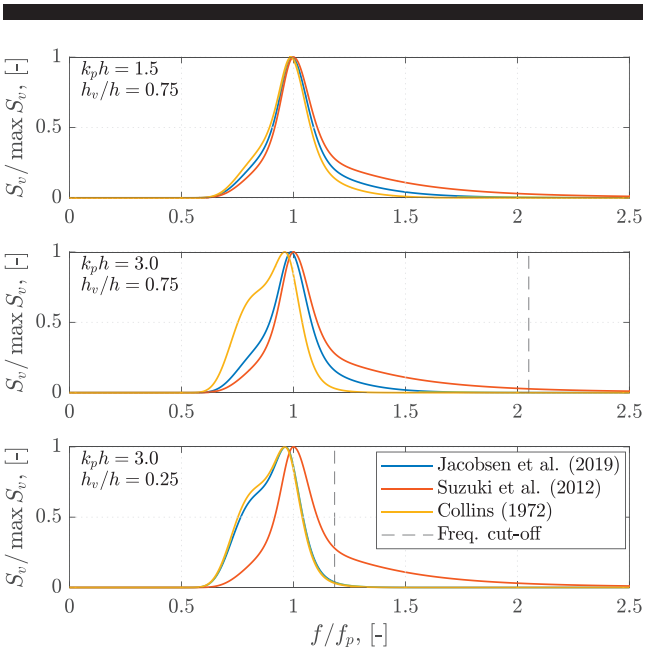

Figure 1. Comparison of the normalized dissipation, $S_v/\max S_v$, for the three dissipation models for a JONSWAP spectrum with a peak enhancement factor of 3.3. The cut-off frequency is defined as $f_{co}^2 = g/(4\pi(h - h_v))$. (Top) $k_p h = 1.5$, $h_v/h = 0.75$, and $f_{co}/f_p = 3.04$. (Middle) $k_p h = 3.0$, $h_v/h = 0.75$, and $f_{co}/f_p = 2.05$. (Bottom) $k_p h = 3.0$, $h_v/h = 0.25$, and $f_{co}/f_p = 1.18$.

expectations, since $S_{v,S-12}$ and $S_{v,J-19}$ become identical when a single wave period is applied. This also implies that the two formulations are identical to Dalrymple, Kirby, and Hwang (1984) for simulations with a single frequency and direction.

Comparison with Analytical Model

Jacobsen, McFall, and Van der A (2019) demonstrated theoretically that the bulk dissipation ratio, $\langle S_{v,S-12} \rangle_{\sigma,\theta} / \langle S_{v,J-19} \rangle_{\sigma,\theta}$, for the same constant drag coefficient is neither unity nor a constant, since the dissipation ratio depends on the stem-height-to-water-depth ratio (h_v/h) and spectral shape. Jacobsen, McFall, and Van der A (2019) analyzed the dissipation ratio for the Joint North Sea Wave Project (JONSWAP) spectrum and three peak enhancement factors, but any spectral shape is applicable in their model (*e.g.*, Pierson-Moskowitz, JONSWAP, TMA, or site-specific). The dissipation ratio is presented in Figure 2 (top) for a JONSWAP spectrum with a peak enhancement factor of 3.3, where the analytical predictions by Jacobsen, McFall, and Van der A (2019) are plotted with numerical predictions from SWAN. The numerical dissipation ratio is evaluated in the very first computational cell, since the transformation in the wave spectra would otherwise invalidate a comparison between analytical and numerical predictions. For this reason, C_D is varied in the range of 0.01–1.00 between cases (sets of $k_p h$ and h_v/h) such that the significant wave height decreased less than 0.2% in the first cell, *i.e.* insignificant spectral transformation and a valid comparison between all model predictions. The SWAN simulations were performed with 400 frequency bins, a water depth of 10 m, an incident significant wave height of 1.0 m, and a peak period such that $k_p h$ was in the range of 0.3 to

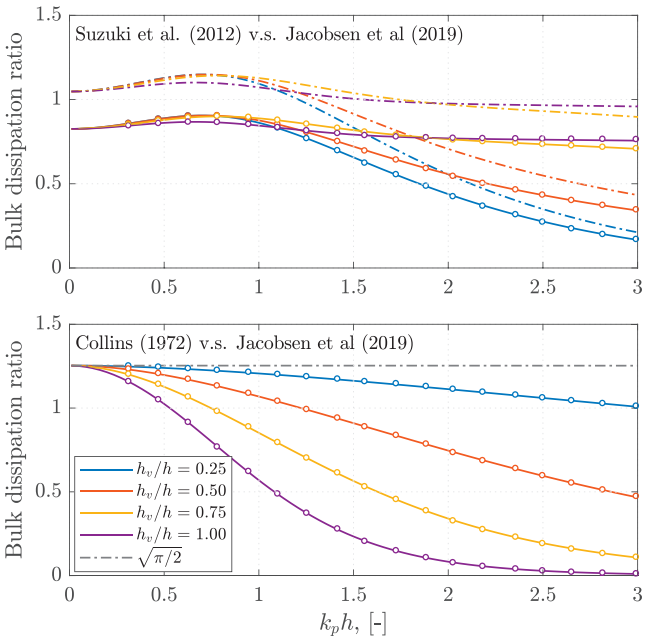

Figure 2. (Top) Comparison between the analytical dissipation ratio ($\langle S_{v,S-12}\rangle_{\sigma,\theta}/\langle S_{v,J-19}\rangle_{\sigma,\theta}$) and the numerical equivalent based on SWAN. Markers: Numerical predictions. Full lines: Analytical predictions with $\tilde{\sigma}$ based on $T_{m0,1}$. Dashed lines: Analytical predictions with $\tilde{\sigma}$ based on $T_{m-1,0}$ as originally documented in Suzuki *et al.* (2012). The dashed lines follow from Jacobsen, McFall, and Van der A (2019), their figure 5B. (Bottom) Comparison between the analytical dissipation ratio ($\langle S_{v,C-72}\rangle_{\sigma,\theta}/\langle S_{v,J-19}\rangle_{\sigma,\theta}$) and the numerical equivalent based on SWAN.

3.0. Intuitively, $k_p h = 3.0$ conflicts with the abundance of vegetation in shallow water depths, though as an example, $k_p h = \{0.3, 3\}$ corresponds to $T_p = \{9.6, 1.6\}$ s in 2 m of water depth and $T_p = \{21, 3.7\}$ s in 10 m of water depth, so the studied range of $k_p h$ covers storm conditions (small $k_p h$) to daily mild conditions (large $k_p h$). Both storm and mild conditions are relevant to incorporate in long-term morphological models that capture both erosion and recovery of the shoreface.

Figure 2 (top) shows that the bulk dissipation differs considerably between the Suzuki *et al.* (2012) and Jacobsen, McFall, and Van der A (2019) models. This is discussed in detail in Jacobsen, McFall, and Van der A (2019), which made the following key observations: (i) The dissipation ratio differs from 1 for vanishing $k_p h$, because $\tilde{\sigma}$ and $\tilde{k}$ do not fulfill the linear dispersion relation. (ii) The dissipation ratio is smallest for short waves (large $k_p h$) and small h_v/h, because the choice of representative frequency is most important for those conditions. Figure 2 (top) further demonstrates that both explicit dissipation models have been correctly implemented, as there is a one-to-one correspondence between the SWAN predictions and the analytical predictions for $\tilde{\sigma}$ based on $T_{m0,1}$. It was furthermore verified (not shown) that a case with $h_v > h$ yields results identical to a case with $h_v = h$, *i.e.* emergent vegetation does not lead to erroneous dissipation. As mentioned in the "Methods" section, the original documentation by Suzuki *et al.* (2012) stated the characteristic frequency to be based on $T_{m-1,0}$, and the corresponding analytical prediction for the dissipation ratio is included in Figure 2 as dashed lines. The two sets of lines are not simply offset by a common factor, see, *e.g.*, the lines for $h_v/h = 0.25$.

The bottom panel in Figure 2 depicts the dissipation ratio $\langle S_{v,C-72}\rangle_{\sigma,\theta}/\langle S_{v,J-19}\rangle_{\sigma,\theta}$ in which $C_f = C_D b_v N_v h_v$ for the Collins model (the factor h_v essentially assumes that the near-bed velocities are uniformly distributed over the water depth). First, the analytical and numerical predictions match, and they both converge to $\sqrt{\pi/2}$ for vanishing $k_p h$. The value $\sqrt{\pi/2}$ follows directly from the ratio between Equations (2) and (8) with the above choice of C_f. Second, the inverse behavior for the two explicit models is found, namely, that the bulk dissipation ratio decreases with increasing h_v/h, and the Collins (1972) and Jacobsen, McFall, and Van der A (2019) models are identical for all $k_p h$ in the limit of vanishing vegetation height. The convergence of the Collins (1972) and Jacobsen, McFall, and Van der A (2019) models for small k_p is also reflected in their frequency-distribution (see Figure 1). Quantification of the resulting differences in terms of spectral transformation over a canopy is addressed in the next section.

Comparison with Experiments

The Jacobsen, McFall, and Van der A (2019) dissipation model describes to what extent the low- or high-frequency energy is dissipated due to the frequency-dependent velocity profile (Equation (8)). On the other hand, the relative dissipation rate over frequencies is fixed for the Suzuki *et al.* (2012) dissipation model (see "Methods" section). This means that both models will likely require different values of the drag parameter C_d. Furthermore, the spectral transformation will also differ, and as a consequence so will the spectral wave period statistics. An evaluation of the spectral transformation is performed next, where numerical predictions are compared to experimental data. In addition to the explicit dissipation models, the implicit dissipation model of Collins (1972) is also applied to highlight the debate on implicit *versus* explicit modeling.

The data of wave attenuation is taken from a laboratory experiment by the U.S. Army Corps of Engineers, focusing on the velocity distribution in a 22.25 m long canopy constructed with wooden dowels, *i.e.* mimicking submerged and emergent canopies. Extensive analysis of the physical model will be documented in subsequent manuscripts. In the present work, 21 experiments with irregular waves are used. The canopy consists of 44.4 cm long birch wooden dowels with a diameter of 9.5 mm, and the density is 625 stems/m^2. The wave flume is 45.7 m long, 1 m deep, 1 m wide and it is equipped with a piston-type wave paddle with active reflection compensation. The wave height was recorded at 16 locations along the flume, with 10 of the submillimeter accuracy capacitance wave gauges within the canopy. An overview of the experimental setup is shown in Figure 3. The water depths ranged from 0.40 m (emergent vegetation) to 0.7 m with increments of 0.1 m. Wave periods from 1.1 s to 2.1 s with wave heights from 0.01 m through 0.11 m were applied at the paddle, and the spectral shape followed JONSWAP with a peak enhancement factor of 3.3. A single steering signal consisting of 250 irregular waves

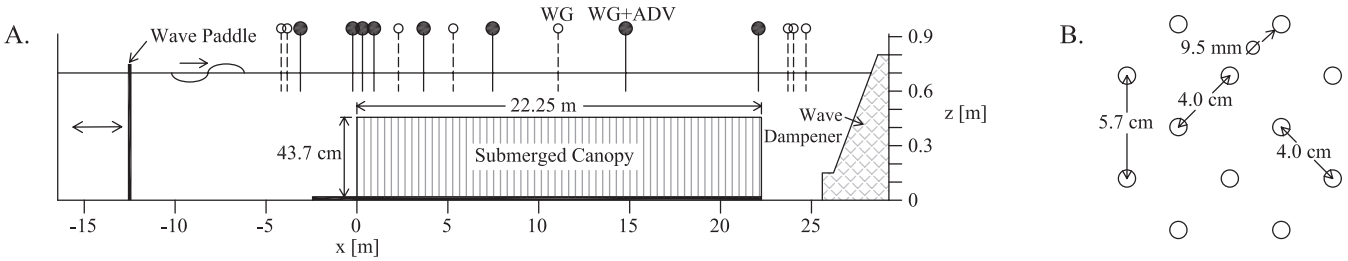

Figure 3. (A) Experimental configuration with location of wave gauges (WG). (B) Schematic of the canopy stem array.

was repeated four times after each other. All wave conditions were nonbreaking (see Table 1).

A SWAN model of the entire flume was set up with a constant water depth and a spatially distributed vegetation (Figure 3), 122 frequency bins over the range 0.03 Hz to 2.5 Hz, and a horizontal resolution of 0.01 m. The spatial resolution is considerably smaller than commonly applied for large-scale spectral modeling, and it was adopted for the sake of comparison with the laboratory setting. The measured wave spectrum in front of the canopy is used as input in SWAN to achieve a one-to-one correspondence between the experiments and model simulations. The parameters C_d and C_f were calibrated for the three dissipation models such that the simulated wave height at the end of the canopy ($x = 22.5$ m) matched the experimental data; the latter taken as the average wave height over the last three wave gauges outside the canopy. The calibrated C_d and C_f parameters are documented in Table 1. The accuracy of this approach is such that the incident wave height is within 1% accuracy and the wave height at the end of the canopy is within 2% of the measured wave height (except for IR31 with the implicit model, where it was not possible to reach the required level of dissipation; here, the low-frequency part of the spectrum was dissipated, where after the wave height remained consistently too large over the remainder of the canopy).

Examples of measured significant wave height (H_{m0}) and spectral wave periods ($T_{m0,1}$ and $T_{m-1,0}$), and the numerical predictions are shown in Figure 4 for cases IR09 and IR36. The wave height decay for the two explicit models is almost identical, while the implicit Collins (1972) model has a steeper decay at the start of the canopy ($x = 0$ m), especially for the emergent case. This steep decay is due to the depletion of energy at low frequencies and the dissipation then stops, since the remaining energy on higher frequencies does not interact with the bed. The measured spectral wave periods $T_{m0,1}$ and $T_{m-1,0}$ decrease for the submerged vegetation case (IR09) and increase for the emergent case (IR36) over the canopy. The implicit model consistently results in a decrease in the spectral wave periods over the canopy, while the explicit model of Suzuki *et al*. (2012) results in an increase of the spectral wave periods over the canopy in all cases. The explicit model of Jacobsen, McFall, and Van der A (2019) provides the correct sign of the change in wave period. The explanation is found in the dissipation formulation, where Suzuki *et al*. (2012) does not incorporate a frequency cut-off f_{co} (at which the waves are too short to feel the vegetation), so excessive dissipation is located at the higher frequencies and thus leads to an increase in wave

Table 1. *Overview of test conditions at the wave paddle and implemented drag/friction coefficients.*

Case name	h(m)	h_v/h	H_{m0}(m)	T_p(s)	k_ph	Suzuki C_D	Jacobsen C_D	Collins C_f
IR06	0.7	0.634	0.072	1.5	1.411	1.73	1.42	7.4
IR07	0.7	0.634	0.086	1.7	1.179	1.62	1.32	6.0
IR08	0.7	0.634	0.010	1.9	1.016	1.55	1.32	5.3
IR09	0.7	0.634	0.110	2.1	0.895	1.52	1.30	4.7
IR11	0.6	0.740	0.056	1.3	1.561	1.75	1.50	15.0
IR12	0.6	0.740	0.069	1.5	1.261	1.60	1.35	9.5
IR13	0.6	0.740	0.082	1.7	1.062	1.54	1.31	7.4
IR14	0.6	0.740	0.095	1.9	0.921	1.52	1.34	6.3
IR15	0.6	0.740	0.106	2.1	0.815	1.47	1.35	5.4
IR21	0.5	0.888	0.041	1.1	1.764	1.58	1.68	220.0
IR22	0.5	0.888	0.053	1.3	1.359	1.50	1.55	45.0
IR23	0.5	0.888	0.065	1.5	1.111	1.44	1.48	18.0
IR24	0.5	0.888	0.077	1.7	0.944	1.42	1.47	11.5
IR25	0.5	0.888	0.088	1.9	0.823	1.38	1.44	8.0
IR26	0.5	0.888	0.099	2.1	0.731	1.40	1.48	6.5
IR31	0.4	1.110	0.039	1.1	1.477	2.30	2.55	10000.0
IR32	0.4	1.110	0.050	1.3	1.160	1.78	1.90	150.0
IR33	0.4	1.110	0.060	1.5	0.961	1.60	1.75	25.0
IR34	0.4	1.110	0.070	1.7	0.823	1.50	1.65	11.5
IR35	0.4	1.110	0.080	1.9	0.722	1.40	1.55	7.0
IR36	0.4	1.110	0.090	2.1	0.643	1.43	1.59	5.8

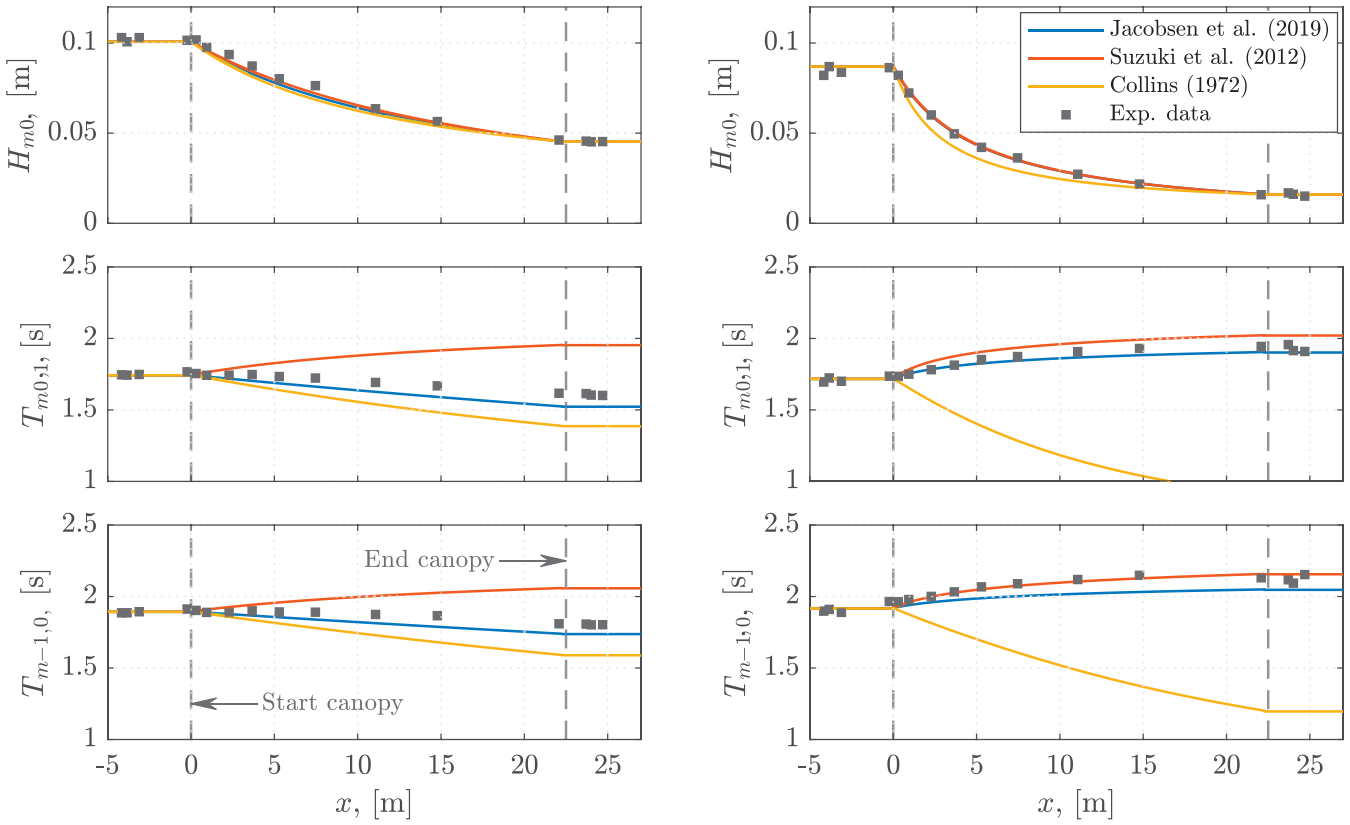

Figure 4. Comparison between the experimental data and three dissipation models available in SWAN. (Left) Test case IR09. (Right) Test case IR36.

periods, while the model by Collins (1972) assumes dissipation by bottom friction, so the high frequencies are subject to too little dissipation, since the vertical structure of the vegetation is omitted. The Suzuki *et al.* (2012) model could partially be improved by setting the dissipation to zero for $f > f_{co}$. This is only a partial improvement, since the assumption of a proportional distribution of the dissipation is still invalid, which is easily observed from the bottom panel in Figure 1.

The spectra through the canopy are shown in Figure 5 for cases IR06 ($k_p h = 1.411; h_v/h = 0.634$), IR31 ($k_p h = 1.477$; $h_v/h = 1.110$), and IR36 ($k_p h = 0.643$; $h_v/h = 1.110$). All three dissipation methods match the experimental data before the canopy as per design. As was similarly observed in Figure 1, the Collins (1972) model dissipates more spectral energy from the lower frequencies, which is most apparent in the IR31 case, where all the energy is depleted for $f < 1.3$ Hz, highlighting that modifying the friction factor will not improve the results. The Jacobsen, McFall, and Van der A (2019) and Suzuki *et al.* (2012) models are essentially identical for the two emergent cases, but for the submerged vegetation case (IR06), the differences between models are clearer. At the end of the canopy, both models similarly match the experimental data for frequencies lower than the peak frequency: Suzuki *et al.* (2012) overestimates the energy in the peak frequency, and Jacobsen, McFall, and Van der A (2019) underestimates it. The Jacobsen, McFall, and Van der A (2019) model captures the spectral energy above the peak frequency better than the Suzuki *et al.* (2012) and Collins (1972) models, which underpredict and overpredict, respectively. This is ascribed to the improved frequency-dependent dissipation technique of the Jacobsen, McFall, and Van der A (2019) model.

The wave periods at the end of the canopy and the change in the wave periods over the length of the canopy are depicted in Figure 6 for all 21 tests. The trends discussed in relation to Figure 4 are recognized, namely, that Suzuki *et al.* (2012) and Collins (1972) exhibit a bias toward larger and smaller wave periods, respectively, while the method by Jacobsen, McFall, and Van der A (2019) correctly predicts the sign and magnitude of the change in spectral wave periods over the length of the canopy. Remaining differences between measured and predicted wave periods could be explained by field observations that C_d is frequency dependent (Jadhav, Chen, and Smith, 2013).

Finally, the tuned value of C_d for the two explicit dissipation models is discussed. Figure 7 depicts C_d as a function of the Keulegan-Carpenter number, KC, and also includes the analytical derivation of C_d following the approach by Mendez and Losada (2004). Their method is commonly applied in the derivation of drag coefficient from wave attenuation data (see, *e.g.*, Anderson and Smith, 2014; Möller *et al.*, 2014). The number $KC = U_m T_p/d$, where U_m is the average orbital velocity over the vegetation height following linear wave theory, with H_{m0} and T_p as wave parameters. The tuned C_d

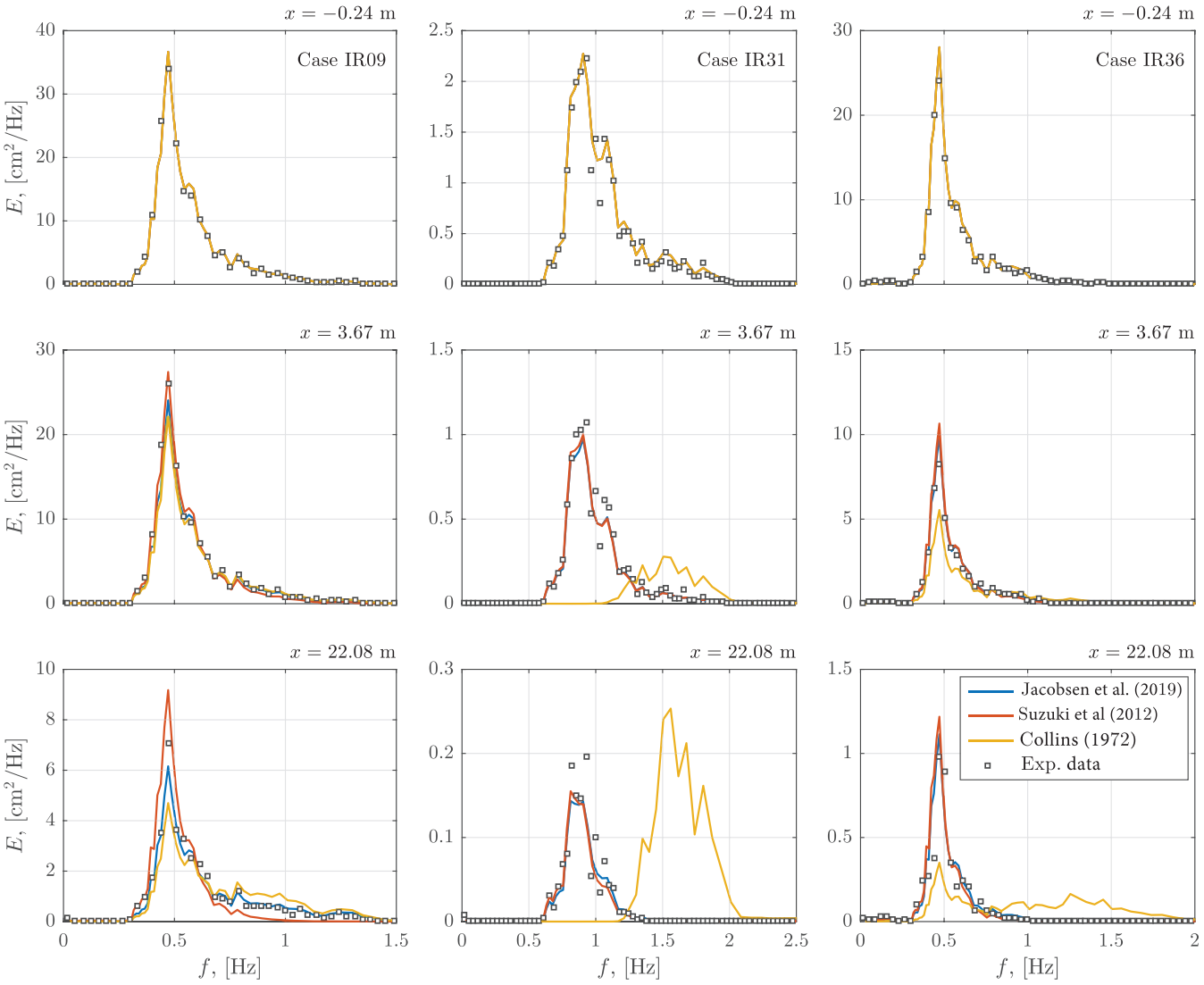

Figure 5. Comparison of the spectral transformation through the canopy for cases IR09, IR31, and IR36.

differs between the Suzuki *et al*. (2012) and Jacobsen, McFall, and Van der A (2019) models, a property that was already predicted theoretically by Jacobsen, McFall, and Van der A (2019). This demonstrates that the interchangeability of C_d between models is not possible. Additionally, the large spread in drag coefficients observed between individual tests calls for a better approach for its determination, since the quantitative predictive skill of wave transformation with considerable dissipation due to vegetation is otherwise not achievable without validation data (unless the risk of large errors can be accepted).

DISCUSSION

The application of both implicit and explicit dissipation models for aquatic vegetation allows for quantitative discussions. The ongoing debate (*e.g.*, Baron-Hyppolite *et al*., 2019; Nowacki, Beudin, and Ganju, 2017) is based on frequency-dependent implicit models and an explicit model based on the bulk parameters representing a characteristic frequency. These model choices (see Figures 4 and6) lead to a bias in the transformation in the wave periods to either smaller (implicit) or larger (explicit) wave periods. Consequently, for vegetation with small h_v/h, an implicit model should be preferred, while the explicit model with a characteristic frequency should be applied for large h_v/h. These two scenarios reflect the works by Nowacki, Beudin, and Ganju (2017) with submerged vegetation and Baron-Hyppolite *et al*. (2019) with (near-) emergent vegetation. The introduction of the frequency-dependent explicit dissipation model of Jacobsen, McFall, and Van der A (2019) in SWAN reduces the need to choose the most appropriate model for a given situation, since it naturally bridges these two extremes.

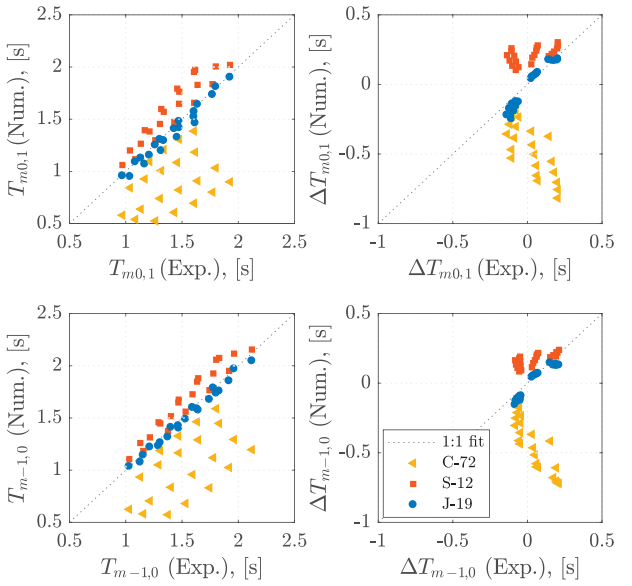

Figure 6. Comparison between experimental and numerical predictions of wave periods. (Upper-left) $T_{m0,1}$ at the end of the canopy. (Upper-right) Change in $T_{m0,1}$ over the 22.5 m long canopy. (Bottom-left) $T_{m-1,0}$ at the end of the canopy. (Bottom-right) Change in $T_{m-1,0}$ over the canopy.

Note that the bias in the transformation in the wave period will affect quantitative estimates of overtopping of coastal structures, since overtopping is a function of, among other things, the spectral wave period $T_{m-1,0}$ (EurOtop, 2018). This effect has currently not been included in studies on wave load reduction by vegetated foreshores such as salt marshes (*e.g.*, Vuik *et al.*, 2016).

The experimental campaign was conducted using a rigid stem canopy. Vegetation comes in a range of rigidity from the essentially rigid (mangroves or reeds under mild-weather conditions) to highly flexible seagrasses undergoing large displacements (Lei and Nepf, 2019; Luhar and Nepf, 2016). The present effort focused on the existing and newly implemented wave energy dissipation term due to vegetation in SWAN, which is why it is deemed sound to use a controlled

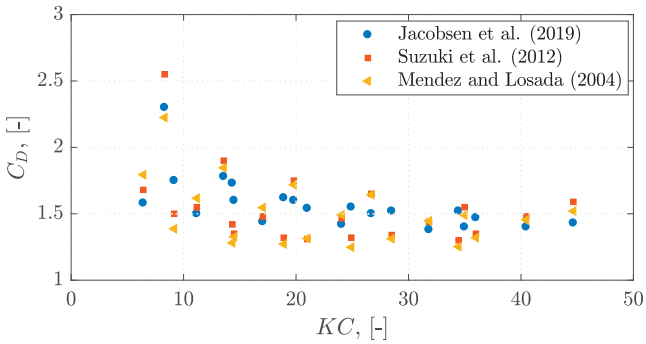

Figure 7. The drag coefficients for three explicit dissipation models.

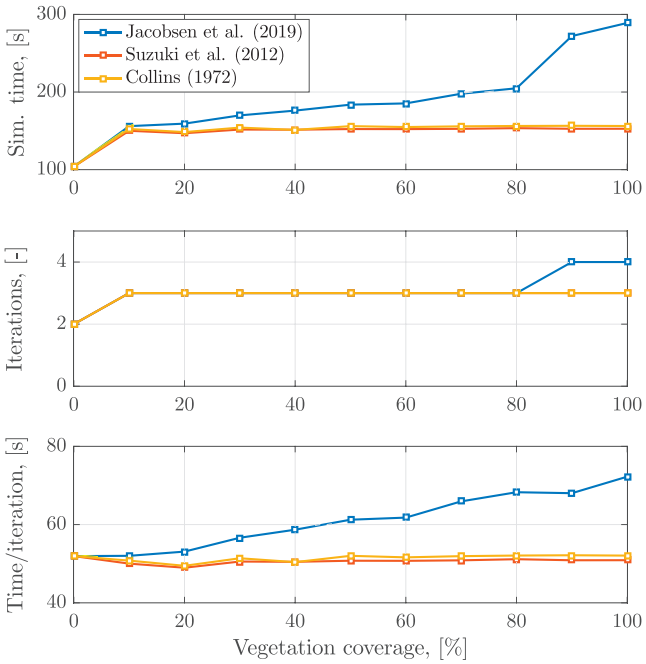

Figure 8. Comparison of the computational cost for the three dissipation models based on case IR06 as a function of the vegetation covered. (Top) Total computational time. (Middle) SWAN iterations. (Bottom) Time per iteration.

laboratory experiment with rigid stem as a canopy mimic. Nonetheless, the authors would welcome future advances of large-scale spectral wave models, where the flexibility of vegetation is accounted for through, *e.g.*, the effective length concept (Lei and Nepf, 2019).

The Jacobsen, McFall, and Van der A (2019) model is shown to provide a better prediction of the spectral transformation through a canopy, however, it does come with a computational overhead. This is quantified for case IR06, where the degree of vegetation coverage is varied from 0% to 100% and the computational time is depicted in Figure 8 for all models. The Collins (1972) and Suzuki *et al.* (2012) models effectively show identical computational performance given their simple formulation, while the vertical integration in Jacobsen, McFall, and Van der A (2019) introduces an overhead that increases with the vegetation coverage. However, it is expected that most large-scale, regional models have a small vegetation coverage, so practically the overhead will be acceptable.

CONCLUSIONS

The Jacobsen, McFall, and Van der A (2019) spectral energy dissipation model has now been implemented in SWAN and released with version 41.31B. Results show that the frequency-dependent Jacobsen, McFall, and Van der A (2019) model has quantitatively better predictive skill than explicit models based on bulk wave characteristics, but there is still a key research question related to the *a priori* selection of an appropriate drag coefficient. The accuracy of such a selection procedure should be related to the general uncertainty in vegetation properties

(density, thickness, height, flexibility, and seasonal effects), which can only be coarsely approximated in most practical engineering projects. This means that sensitivity studies and possibly probabilistic approaches are still most suitable for the engineering application for flood safety.

Finally, the current model validation is entirely based on academic test cases and laboratory flume experiments with a much finer spatial and frequency resolution than applied in typical engineering applications. Therefore, analysis of the performance of the different vegetation models for field experiments is recommended. Preferably, these experiments concern storm conditions with a large range of water depths to enable a reflection on the relevance of the mutual differences from the perspective of flood risk reduction by vegetated foreshores.

ACKNOWLEDGMENTS

Funding from Deltares' strategic research program on Nature-based solutions is greatly appreciated. The corresponding author appreciates the funding from the international collaboration program with Rijkswaterstaat, The Netherlands. The experimental campaign was supported by the U.S. Army Corps of Engineers through the Coastal Inlet Research Program, Regional Sediment Management Program, Engineering with Nature initiative, and Flood and Coastal Systems Program.

LITERATURE CITED

Anderson, M.E. and Smith, J.M., 2014. Wave attenuation by flexible, idealized salt marsh vegetation. *Coastal Engineering*, 83, 82–92.

Ascencio, J.A., 2020. Spectral Wave Dissipation by Vegetation: A New Frequency Distributed Dissipation Model in SWAN. Delft, Netherlands: Delft University of Technology, Master's thesis, 113p.

Baron-Hyppolite, C.; Lashley, C.H.; Garzon, J.; Miesse, T.; Ferreira, C., and Bricker, J.D., 2019. Comparison of implicit and explicit vegetation representations in SWAN hindcasting wave dissipation by coastal wetlands in Chesapeake Bay. *Geosciences*, 9(1), 8.

Booij, N.R.R.C.; Ris, R.C., and Holthuijsen, L.H., 1999. A third-generation wave model for coastal regions: 1. Model description and validation. *Journal of Geophysical Research: Oceans*, 104(C4), 7649–7666.

Chang, C.W.; Liu, P.L.F.; Mei, C.C., and Maza, M., 2017. Modeling transient long waves propagating through a heterogeneous coastal forest of arbitrary shape. *Coastal Engineering*, 122, 124–140.

Chen, Q. and Zhao, H., 2012. Theoretical models for wave energy dissipation caused by vegetation. *Journal of Engineering Mechanics*, 138(2), 221–229.

Chen, H. and Zou, Q.P., 2019. Eulerian–Lagrangian flow-vegetation interaction model using immersed boundary method and OpenFOAM. *Advances in Water Resources*, 126, 176–192.

Collins, J.I., 1972. Prediction of shallow-water spectra. *Journal of Geophysical Research*, 77(15), 2693–2707.

Dalrymple, R.A.; Kirby, J.T., and Hwang, P.A., 1984. Wave diffraction due to areas of energy dissipation. *Journal of Waterway, Port, Coastal, and Ocean Engineering*, 110(1), 67–79.

EurOtop, 2018. *EurOtop: Manual on Wave Overtopping of Sea Defences and Related Structures. An Overtopping Manual Largely Based on European Research, but for Worldwide Application*, 2nd edition. Van der Meer, J.W.; Allsop, N.W.H.; Bruce, T.; De Rouck, J.; Kortenhaus, A.; Pullen, T.; Schüttrumpf, H.; Troch, P., and Zanuttigh, B., 304p. www.overtopping-manual.com

Holthuijsen, L.H., 2007. *Waves in Oceanic and Coastal Waters*. Cambridge, U.K.: Cambridge Univ. Press, 387p.

Hu, J.; Mei, C.C.; Chang, C.W., and Liu, P.L., 2021. Effect of flexible coastal vegetation on waves in water of intermediate depth. *Coastal Engineering*, 168, 103937.

Jacobsen, N.G.; McFall, B.C., and van der A, D.A., 2019. A frequency distributed dissipation model for canopies. *Coastal Engineering*, 150, 135–146.

Jadhav, R.S.; Chen, Q., and Smith, J.M., 2013. Spectral distribution of wave energy dissipation by salt marsh vegetation. *Coastal Engineering*, 77, 99–107.

Lei, J. and Nepf, H.M., 2019. Wave damping by flexible vegetation: Connecting individual blade dynamics to the meadow scale. *Coastal Engineering*, 147, 138–148.

Luhar, M. and Nepf, H.M., 2016. Wave-induced dynamics of flexible blades. *Journal of Fluids and Structures*, 61, 20–41.

Mendez, F.J. and Losada, I.J., 2004. An empirical model to estimate the propagation of random breaking and nonbreaking waves over vegetation fields. *Coastal Engineering*, 51(2), 103–118.

Möller, I.; Kudella, M.; Rupprecht, F.; Spencer, T.; Paul, M.; Van Wesenbeeck, B.K.; Wolters, G.; Jensen, K.; Bouma, T.J.; Miranda-Lange, M., and Schimmels, S., 2014. Wave attenuation over coastal salt marshes under storm surge conditions. *Nature Geoscience*, 7(10), 727–731.

Nowacki, D.J.; Beudin, A., and Ganju, N.K., 2017. Spectral wave dissipation by submerged aquatic vegetation in a back-barrier estuary. *Limnology and Oceanography*, 62(2), 736–753.

Ozeren, Y.; Wren, D.G., and Wu, W., 2014. Experimental investigation of wave attenuation through model and live vegetation. *Journal of Waterway, Port, Coastal, and Ocean Engineering*, 140(5), 04014019.

Suzuki, T.; Hu, Z.; Kumada, K.; Phan, L.K., and Zijlema, M., 2019. Non-hydrostatic modeling of drag, inertia and porous effects in wave propagation over dense vegetation fields. *Coastal Engineering*, 149, 49–64.

Suzuki, T.; Zijlema, M.; Burger, B.; Meijer, M.C., and Narayan, S., 2012. Wave dissipation by vegetation with layer schematization in SWAN. *Coastal Engineering*, 59(1), 64–71.

Van Rooijen, A.; Lowe, R.; Rijnsdorp, D.P.; Ghisalberti, M.; Jacobsen, N.G., and McCall, R., 2020. Wave-driven mean flow dynamics in submerged canopies. *Journal of Geophysical Research: Oceans*, 125(3), p.e2019JC015935.

Van Rooijen, A.A.; McCall, R.T.; Van Thiel de Vries, J.S.M.; Van Dongeren, A.R.; Reniers, A.J.H.M., and Roelvink, J.A., 2016. Modeling the effect of wave-vegetation interaction on wave setup. *Journal of Geophysical Research: Oceans*, 121(6), 4341–4359.

Vuik, V.; Jonkman, S.N.; Borsje, B.W., and Suzuki, T., 2016. Nature-based flood protection: The efficiency of vegetated foreshores for reducing wave loads on coastal dikes. *Coastal Engineering*, 116, 42–56.

Vuik, V.; Van Vuren, S.; Borsje, B.W.; van Wesenbeeck, B.K., and Jonkman, S.N., 2018. Assessing safety of nature-based flood defenses: Dealing with extremes and uncertainties. *Coastal Engineering*, 139, 47–64.

WAMDI Group, 1988. The WAM model—A third generation ocean wave prediction model. *Journal of Physical Oceanography*, 18(12), 1775–1810.

Zhu, L.; Huguenard, K.; Zou, Q.P.; Fredriksson, D.W., and Xie, D., 2020. Aquaculture farms as nature-based coastal protection: Random wave attenuation by suspended and submerged canopies. *Coastal Engineering*, 160, 103737.